

To appear in the *Astronomical Journal*

New X-ray Detections of WNL Stars

Stephen L. Skinner

*Center for Astrophysics and Space Astronomy (CASA), Univ. of Colorado, Boulder, CO
80309-0389; email: Stephen.Skinner@colorado.edu*

Svetozar A. Zhekov

Space and Solar-Terrestrial Research Institute, Moskovska str. 6, Sofia-1000, Bulgaria

Manuel Güdel

Dept. of Astronomy, Univ. of Vienna, Türkenschanzstr. 17, A-1180 Vienna, Austria

Werner Schmutz

*Physikalisch-Meteorologisches Observatorium Davos (PMOD), Dorfstrasse 33, CH-7260
Davos Dorf, Switzerland*

Kimberly R. Sokal

Dept. of Astronomy, Univ. of Virginia, P.O. Box 400325, Charlottesville, VA 22904-4325

ABSTRACT

Previous studies have demonstrated that putatively single nitrogen-type Wolf-Rayet stars (WN stars) without known companions are X-ray sources. However, almost all WN star X-ray detections so far have been of earlier WN2 - WN6 spectral subtypes. Later WN7 - WN9 subtypes (also known as WNL stars) have proved more difficult to detect, an important exception being WR 79a (WN9ha). We present here new X-ray detections of the WNL stars WR 16 (WN8h) and WR 78 (WN7h). These new results, when combined with previous detections, demonstrate that X-ray emission is present in WN stars across the full range of spectral types, including later WNL stars. The two WN8 stars observed to date (WR 16 and WR 40) show unusually low X-ray luminosities (L_x) compared to other WN stars, and it is noteworthy that they also have the lowest terminal wind speeds (v_∞). Existing X-ray detections of about a dozen WN stars reveal a trend of increasing L_x with wind luminosity $L_{wind} = \frac{1}{2}\dot{M}v_\infty^2$, suggesting that wind kinetic energy may play a key role in establishing X-ray luminosity levels in WN stars.

Subject headings: stars: individual (WR 16; WR 78; WR 79a) — stars: Wolf-Rayet — X-rays: stars

1. Introduction

The detection of X-ray emission from Wolf-Rayet (WR) stars was one of the many notable discoveries of the *Einstein Observatory* (Seward et al. 1979; Pollock 1987). Subsequent studies have broadened our knowledge of the X-ray properties of WR stars but the underlying physical mechanisms ultimately responsible for their X-ray emission are still not well understood. Most current theoretical models attribute the X-ray emission of WR stars (and O-type stars) to thermal plasma produced in shocks that form in their powerful supersonic winds. WR stars have typical terminal wind speeds $v_\infty \sim 1000 - 5000 \text{ km s}^{-1}$ and mass-loss rates $\dot{M} \sim 10^{-5} M_\odot \text{ yr}^{-1}$. It has also been suggested that WR stars might produce non-thermal X-rays via such processes as inverse-Compton scattering, synchrotron emission, or nonthermal bremsstrahlung (Pollock 1987; Chen & White 1991). However, most WR stars detected so far show line-dominated X-ray spectra that can be acceptably fitted by thermal models. But, nonthermal emission has not yet been ruled out in a few cases (e.g. WR 142; Sokal et al. 2010).

Several different shock-related processes could in principle lead to thermal X-ray emission in WR stars. First, soft X-rays ($kT < 1 \text{ keV}$) may be produced in shocks embedded in the outflowing wind that form as a result of the line-driven instability (Lucy & White 1980; Lucy 1982; Feldmeier et al. 1997; Gayley & Owocki 1995). This mechanism may be responsible for the soft X-ray emission detected in some O-type stars (Cassinelli et al. 2001; Kahn et al. 2001). But, all WR stars detected so far show a harder component ($kT \gtrsim 2 \text{ keV}$) in addition to a soft component that is usually present. The hard component is not expected if the emission arises solely from line-driven instability shocks. Second, a sufficiently strong magnetic field could confine the wind and channel it into two opposing streams which collide near the magnetic equator, forming a magnetically-confined wind shock (MCWS). This mechanism is capable of producing hard X-rays ($kT \gtrsim 2 \text{ keV}$) and may be relevant to X-ray production in young magnetic OB stars such as $\theta^1 \text{ Ori C}$ (Babel & Montmerle 1997b; Gagné et al. 2005) and $\sigma \text{ Ori E}$ (Skinner et al. 2008). However, very strong surface magnetic fields would be needed to confine the more powerful winds of WR stars (ud-Doula & Owocki 2002; Skinner et al. 2010, hereafter S10), and observational evidence for strong magnetic fields on WR stars is currently lacking. Thus, the question of whether the MCWS mechanism operates in WR stars remains open. Finally, in the case of WR + OB binary systems, hard X-rays ($kT \gtrsim 2 \text{ keV}$) can originate in the region between the two stars where

the interaction of their winds results in a colliding wind (CW) shock (Prilutskii & Usov 1976; Luo et al. 1990; Stevens et al. 1992; Usov 1992). Hot X-ray plasma that is thought to arise at least partially in a CW shock has now been detected in grating spectra of several X-ray bright WR + OB binaries (γ^2 Vel: Skinner et al. 2001; Schild et al. 2004; WR 140: Pollock et al. 2005; WR 147: Zhekov & Park 2010).

X-ray spectra of WR stars are needed to distinguish between the above possibilities. Although good-quality X-ray grating spectra of a few X-ray bright WR+OB binaries have been obtained (as noted above), the study of putatively single WR stars as a class has been hampered by a general lack of X-ray spectral data. The observational situation has improved considerably during the past few years as a result of the completion of an exploratory X-ray survey of single WR stars with *XMM-Newton* and *Chandra* (S10). Moderate-resolution CCD X-ray spectra are now available for several WN stars but attempts to detect carbon-rich WC stars have so far only yielded upper limits on their X-ray luminosities with typical constraints of $\log L_x < 31.0$ ergs s⁻¹ (Skinner et al. 2006; see also Fig. 9 of S10).

A surprising result of the initial survey was that all detected WN stars showed evidence of hot plasma ($kT_{hot} \gtrsim 2$ keV) in their X-ray spectra. This result is at odds with X-ray production via the line-driven instability mechanism, for which only soft emission is expected. It is thus apparent that other mechanisms are needed to fully explain the origin of X-ray emission in WN stars and, within the current theoretical framework, either the MCWS or CW shock processes could be responsible. However, there is no compelling justification to invoke the CW interpretation because the WN stars in the initial survey sample were selected on the basis of lack of evidence for binarity. The presumption that these stars are indeed single is of course subject to the usual caveat that close companions can escape detection.

In the initial survey, *XMM-Newton* and *Chandra* data for the following detected WN stars were analyzed: WR 2 (WN2), WR 18 (WN4), WR 20b (WN6h), WR 24 (WN6ha), WR 134 (WN6), WR 136 (WN6h), and WR 79a (WN9ha). In addition, archival *ROSAT* data were analyzed for WR 16 (WN8h) and WR 78 (WN7h). Neither of these two WNL stars¹ showed significant X-ray emission (see also Sanders et al. 1985), although a marginal (2σ) excess was noted in hard-band *ROSAT* PSPC² images of WR 78. We present here

¹Nitrogen-rich WR stars with spectral types in the range WN7 - WN9 are referred to as late WN stars, or WNL stars. Those with spectral types of WN2 - WN5 are called early WN stars or WNE stars. WN6 stars are intermediate and may be classified as either WNE or WNL (Crowther 2007). A “h” suffix in the spectral type denotes the presence of hydrogen emission lines in the spectrum.

²The *ROSAT* Position Sensitive Proportional Counter (PSPC) provided energy coverage in the ≈ 0.1 - 2.35 keV energy range but lacked sensitivity at higher energies $E \gtrsim 2.35$ keV. PSPC hard-band images cover the range $E \approx 0.5$ - 2 keV. In contrast, *XMM-Newton* provides coverage to higher energies and we use the

more sensitive *XMM-Newton* observations of WR 16 and WR 78 that were obtained after the results of our initial WN survey were published (S10). These observations are important because they provide additional information on the X-ray properties of WNL subtypes, which comprise $\approx 24\%$ of all WR stars listed in the *VIIth Catalog of Wolf-Rayet Stars* (van der Hucht 2001). WNL stars are believed to be the least chemically-evolved WR stars and some O-type stars probably enter the WR phase as WNL stars (Crowther & Bohannan 1997). WNL stars typically have higher mass-loss rates but lower terminal wind speeds than WNE stars (Table 2 of Crowther 2007). We report here a faint X-ray detection of WR 16 (WN8h) and bright emission including a hot plasma component from WR 78 (WN7h).

2. Observations

The *XMM-Newton* observations are listed in Table 1. The general properties of the WNL stars discussed here are summarized in Table 2 and their X-ray properties are given in Table 3. The targets were selected from the *VIIth WR Catalog* (van der Hucht 2001) based on proximity, low visual extinction, and lack of evidence for binarity. In addition to the new detections of WR 16 and WR 78, we also include data from our previous *XMM-Newton* observation (S10) of the WNL star WR 79a for comparison.

Data were acquired with the European Photon Imaging Camera (EPIC) in full-window mode. EPIC provides charge-coupled device (CCD) imaging spectroscopy from the pn camera (Strüder et al. 2001) and two nearly identical MOS cameras (MOS1 and MOS2; Turner et al. 2001). The EPIC cameras provide energy coverage in the range $E \approx 0.2 - 15$ keV with energy resolution $E/\Delta E \approx 20 - 50$. The MOS cameras provide the best on-axis angular resolution with FWHM $\approx 4.3''$ at 1.5 keV.

Data were reduced using the *XMM-Newton* Science Analysis System (SAS vers. 11.0) using standard procedures including the filtering of raw event data to select good event patterns and removal of data within time intervals of high background radiation. Spectra and light curves were extracted from a circular region of radius $r = 15''$ ($\approx 68\%$ encircled energy) centered on the source, thus capturing most of the source counts while reducing background counts. Background analysis was conducted on circular source-free regions near the source. The SAS tasks *rmfgen* and *arfgen* were used to generate source-specific RMFs and ARFs for spectral analysis. The data were analyzed using the HEASOFT *Xanadu* software package.

energy range $E = 2 - 8$ keV to refer to the *XMM-Newton* hard-band.

3. Results

3.1. WR 16 (= V396 Car = HD 86161)

This WN8h star has the lowest terminal wind speed ($v_\infty \approx 630 - 740 \text{ km s}^{-1}$) of any WN star in our exploratory X-ray survey. The star is surrounded by a cocoon of molecular gas which was probably ejected during a previous evolutionary phase (Marston et al. 1999). Optical variability is present but its cause is not fully understood (Antokhin et al. 1995). An early study attributed the variability to an unseen low-mass companion (Moffat & Niemela 1982) but this interpretation was later called into question (Manfroid et al. 1987). The stellar distance is somewhat uncertain with published values ranging from 2.37 - 4.36 kpc (Crowther et al. 1995; Nugis & Lamers 2000; van der Hucht 2001, Hamann et al. 2006) and we adopt here an intermediate value $d \approx 3.6 \text{ kpc}$.

Visual inspection of energy-filtered EPIC images showed no obvious signs of an X-ray source at the stellar optical position. However, more in-depth image analysis revealed a weak emission excess above the local background level in both the pn and MOS images. We extracted counts (0.3 - 8 keV) within a circular region of radius $15''$ (68% encircled energy) centered on the star in each EPIC detector, and background counts in different source-free regions near the star. After background subtraction we obtained 31 ± 6 net pn counts in 30.0 ks of usable exposure and 24 ± 5 net MOS1+2 (sum of MOS1 and MOS2) in 66.0 ks of usable exposure (33.0 ks per MOS). The faint emission is clearly visible in the contoured MOS1+2 image in Figure 1. Although the statistical significance of the excess is low ($\approx 2\sigma$), its presence in all three EPIC detectors at an offset of $< 1''$ from the *HST* GSC optical position (Table 3) strengthens the conclusion that weak X-ray emission from WR 16 is detected.

The emission is too faint for spectral and timing analysis. However, we used the PIMMS³ simulator to estimate the X-ray luminosity of WR 16 based on the count rates. The pn rate of 1.03 c ks^{-1} gives an unabsorbed luminosity $\log L_X(0.3 - 8 \text{ keV}) = 31.14 [30.77 - 31.30]$ ergs s^{-1} for an assumed distance $d = 3.6 \text{ kpc}$, where the range in square brackets reflects the range of published distances $d = 2.37 - 4.36 \text{ kpc}$. A PIMMS estimate based on the MOS count rate gives a nearly identical unabsorbed value $\log L_X(0.3 - 8 \text{ keV}) = 31.17 [30.80 - 31.33]$ ergs s^{-1} . For the underlying spectrum, we assumed an absorbed two-temperature optically thin thermal plasma (*apec*) with $kT_1 = 0.6 \text{ keV}$ and $kT_2 = 3.5 \text{ keV}$, typical of detected WN stars (S10). We adopted an absorption column density $N_H = 3.7 \times 10^{21} \text{ cm}^{-2}$ based on $A_V = 1.67$ (Table 1) and the Gorenstein (1975) conversion from A_V to N_H . The

³For information on PIMMS (Portable Interactive Multi-Mission Simulator) see <http://cxc.harvard.edu/ciao/ahelp/pimms.html>.

slightly different conversion of Vuong et al. (2003) decreases the upper limit on L_X by 0.05 dex.

The above L_X is the lowest of any WN star detected so far, but the derived value is dependent on the assumed spectral model and absorption. Most WN stars show X-ray absorption in excess of that expected from A_V (S10; see also the results for WR 78 in Sec. 3.2 below). If that is the case for WR 16, then its unabsorbed L_X could be larger than the value inferred above. In this regard, we note that the pn counts for WR 16 are distributed roughly equally between the soft (0.3 - 2 keV) and hard (2 - 8 keV) bands. But, XSPEC simulations show that if the absorption were as low as expected based on A_V , only about $\approx 15\%$ - 20% of the counts would emerge in the hard band. This suggests that excess absorption above that expected from A_V is present in WR 16, but a higher signal-to-noise spectrum would be needed to confirm this. For those WN stars where sufficient counts are available for spectral analysis, the best-fit N_H values are typically ≈ 2.0 - 2.5 times larger than expected from estimates based on A_V (Table 4 of S10). If we assume that is the case for WR 16 then its unabsorbed L_X determined from PIMMS is ≈ 0.10 - 0.15 dex larger than the values quoted above.

3.2. WR 78 (= V919 Sco = HD 151932)

This WN7h star has been included in numerous optical studies and there is fairly good agreement in published stellar parameters when different studies are compared (Table 2). Optical variability has been reported (Vreux et al. 1987; Bratschi & Blecha 1996) but no periodicity that would hint of a companion has been found.

XMM-Newton provides the first unambiguous detection of WR 78 (Fig. 2). The source is quite hard as is apparent from its median photon energy $E_{50} = 2.47$ keV (Table 3). Clear evidence for high-temperature plasma is provided by the detection of the Fe $K\alpha$ emission line complex at 6.67 keV (Fig. 3). This line forms at a characteristic temperature $T \sim 40$ MK. Using pn events in the 0.3 - 8 keV range, the Kolmogorov-Smirnov (KS) test gives a probability of constant count rate $P_{cons} = 0.12$ and a χ^2 test applied to the background-subtracted pn light curve binned at 1000 s intervals gives $P_{cons} = 0.97$. The KS test operates on all detected events within the source extraction region, and thus includes both background and source events. The lower value of P_{cons} based on the KS test may be due to background effects. But, neither the KS test nor χ^2 analysis suggests statistically significant variability for WR 78 during the 26.26 ks (7.3 hours) of usable exposure. Likewise, the other WN stars in the survey have failed to show any clear X-ray variability in observations spanning ≈ 3 - 10 hours (S10).

Acceptable fits of the CCD X-ray spectra of WN stars detected in the initial survey were obtained using a two-temperature (2T) optically thin plasma model consisting of cool (kT_1) and hot (kT_2) plasma components plus a single absorption component (N_H). This model is expressed symbolically as $N_H*(kT_1 + kT_2)$, where parentheses denote that both plasma components are viewed through the same absorption column. Interestingly, this model gives an unacceptable fit of the WR 78 X-ray spectrum as does a simpler 1T model of the form N_H*kT_1 . These single-absorption models fit the spectrum above 2 keV (including the Fe $K\alpha$ line) reasonably well, but generally underestimate the observed flux at energies below 1 keV. A similarly poor fit below 1 keV occurs for other single-absorption models such as a plane-parallel shock model (*vpshock* in XSPEC). In order to obtain an acceptable fit for WR 78, different absorption components were required for the cool and hot components, i.e. a model of the form $N_{H,1}*kT_1 + N_{H,2}*kT_2$.

The acceptable two-absorber model is summarized in Table 4. The inferred plasma temperatures $kT_1 = 0.64$ [0.48 - 0.88; 90% conf.] keV and $kT_2 = 2.27$ [1.63 - 2.90] keV are not substantially different from the WN9h star WR 79a (Sec. 3.3) when 90% confidence ranges are taken into account, but the value of kT_2 is at the low end of the range for all WN stars observed so far (S10). Most of the X-ray flux and emission measure (as gauged by the value of *norm* in Table 4) of WR 78 is associated with the hotter plasma component, which is evidently viewed through much higher absorption than the cool component. The separate contributions of the cool and hot components are shown in the bottom panel of Figure 3. The best-fit absorption values of $N_{H,1} = 1.38$ [1.20 - 1.60] $\times 10^{22}$ cm^{-2} and $N_{H,2} = 6.55$ [4.10 - 10.7] $\times 10^{22}$ cm^{-2} are substantially larger than expected on the basis of visual extinction estimates, since $A_V = 1.55$ mag (Table 2) corresponds to $N_H = 3.4 \times 10^{21}$ cm^{-2} using the conversion of Gorenstein (1975). The two-absorber model for WR 78 gives an unabsorbed X-ray luminosity $\log L_x(0.3 - 8 \text{ keV}) = 32.84$ ergs s^{-1} ($d = 1.99$ kpc; Table 4), which is at the high end of the range for detected WN stars (Fig. 4; S10). However, this value is quite uncertain because of the large dereddening correction. All spectral models that we considered, including simplistic 1T models, give values $\log L_x(0.3 - 8 \text{ keV}) \geq 32.1$ ergs s^{-1} which we consider to be a reliable lower limit.

The most likely cause of the anomalous X-ray absorption is the WR wind. In that case, the higher absorption associated with the hot plasma component suggests that it originates deeper in the wind (closer to the star) where the wind density is higher. A similar conclusion was reached for the WN6h star WR 136 (S10) and for O-type stars studied by Waldron & Cassinelli (2007) and Nazé (2009). In the ideal case of a smooth unclumped wind, the radius of optical depth unity (as measured from the star) decreases toward higher X-ray energies so harder photons are able to escape from smaller radii near the star. Softer X-ray photons produced far out in the wind suffer less wind absorption and can escape whereas any soft

photons produced in deeper denser layers of the wind are absorbed and remain undetected. In the more complex case of an inhomogeneous (clumped) wind, the above picture is not altered substantially if the clumps are optically thin to X-rays but could well be different if dense optically thick clumps are present.

3.3. WR 79a (= HD 152408)

This WN9ha star is the latest WN subtype detected in X-rays so far. It is discussed in more detail in S10 but for comparison we summarize its X-ray properties in Table 3 and give its best-fit spectral parameters in Figure 3. The EPIC pn spectrum of WR 79a is softer than that of WR 78 as evidenced by its lower median photon energy (Table 3) and it is apparent from Figure 3 that the X-ray absorption of WR 79a is less than that of WR 78. The pn spectra of both stars show the high-temperature S XV (2.46 keV) emission line but the very high temperature Fe K α complex (6.67 keV) detected in WR 78 is not seen in WR 79a.

4. Discussion

4.1. What Stellar Parameters Control WN Star X-ray Luminosity?

The fundamental stellar parameters that govern intrinsic X-ray luminosity levels in WR stars have not yet been identified. Good quality X-ray data or useful upper limits exist for only about a dozen putatively single WN stars, so robust statistics and stringent tests for correlations of L_x against stellar parameters are still limited by small sample size. This is in contrast to massive O-type stars, from which WR stars evolve. X-ray data now exist for hundreds of O-type stars and the empirical relation $L_x \sim 10^{-7}L_{bol}$ was already becoming apparent from a large sample of O and early B stars detected in the *ROSAT* All-Sky Survey (Berghöfer et al. 1997).

Based on existing *XMM-Newton* and *Chandra* X-ray data, there is no convincing evidence for a similar $L_x \propto L_{bol}$ relation in putatively single WN stars. Likewise, no evidence for such a relation was found using *ROSAT* data (Wessolowski 1996). As we have already shown (S10), WN stars with similar values of L_{bol} can have L_x values differing by an order of magnitude or more. Most detected WN stars, including WR 78 (Table 4), have $L_x \gtrsim 10^{-7}L_{bol}$ with typical values being $L_x \sim 10^{-6.5}L_{bol}$, as shown in Figure 4. However there are a few WNL stars whose L_x/L_{bol} ratios are at least an order of magnitude lower. Most notable among these is WR 16 (WN8h), for which we obtain $\log L_x/L_{bol} = -8.2 \pm 0.2$ when taking the range of published distances and stellar luminosities into account (Table 2). A similarly

low L_x/L_{bol} ratio is also assured for WR 40 (WN8h) by virtue of its *XMM* non-detection with an X-ray upper limit $\log L_x(0.5 - 10 \text{ keV}) \leq 31.6 \text{ ergs s}^{-1}$ at an assumed distance $d = 3 \text{ kpc}$ (Gosset et al. 2005).

Wind shock models of X-ray emission from massive stars predict that L_x will depend on mass-loss parameters. In the line-driven instability shock model, $L_x \propto \dot{M}^\alpha$ where $\alpha = 1$ for the radiative shock case, $\alpha = 2$ for the adiabatic case, and $\alpha = 0.6$ if the observed $L_x \propto L_{bol}$ scaling relation in O-type stars is to be reproduced (Owocki et al. 2011). From an observational standpoint, there is no clear dependence of L_x on \dot{M} for WN stars. In particular WR 2 (WN2) has one of the lowest mass-loss rates tabulated for WN stars ($\log \dot{M} = -5.4 - -5.3 \text{ M}_\odot \text{ yr}^{-1}$; Nugis & Lamers 2000; Hamann et al. 2006) but its L_x is comparable to that of other WN stars having \dot{M} values an order of magnitude larger. In addition, the two WN8 stars WR 16 and WR 40 are underluminous in X-rays by about an order of magnitude compared to other WN stars with similar mass-loss rates. Thus, mass-loss rate alone is not a reliable predictor of L_x in WN stars.

There is one clue in the existing data that suggests L_x in WN stars may depend on terminal wind speed v_∞ or some function thereof. Specifically, we note that the two observed WN8 stars WR 16 ($v_\infty \approx 630 - 740 \text{ km s}^{-1}$) and WR 40 ($v_\infty \approx 650 - 910 \text{ km s}^{-1}$) have the lowest terminal wind speeds of all WN stars (Hamann et al. 2006; see also Gosset et al. 2005 for WR 40). These two stars also have the lowest L_x values, even though only an upper limit is currently available for WR 40. The WN8h star WR 156 also has a similar low wind speed ($v_\infty \approx 660 \text{ km s}^{-1}$; Hamann et al. 2006) but it has not yet been observed in X-rays. In the absence of a binary companion we expect that any X-ray detection of WR 156 would be quite faint.

The apparent falloff in L_x with decreasing v_∞ suggests that L_x may be related to wind momentum ($= \dot{M}v_\infty$) or wind luminosity $L_{wind} (= \frac{1}{2}\dot{M}v_\infty^2)$. Using data in the initial WN X-ray survey (S10), we already noted a trend of increasing L_x with L_{wind} . The new detections of WR 16 and WR 78 presented here conform to and strengthen this trend (Fig. 5). This trend was not seen in *ROSAT* WN-star data analyzed by Wesselowski (1996), perhaps because *ROSAT* had little sensitivity above $\sim 2 \text{ keV}$ where a significant fraction of the X-ray flux in WN stars emerges. Using the data in Figure 5, the generalized Kendall's tau test gives a correlation probability $P_{corr} = 0.93$. A linear regression fit gives $\log L_x = 0.89(\pm 0.47)\log L_{wind} + 26.41(\pm 0.55)$ where L_x is in units of ergs s^{-1} and L_{wind} in units of $10^{-5}\text{M}_\odot \text{ yr}^{-1} \times (\text{km s}^{-1})^2$. Thus, the regression fit gives a nearly linear dependence $L_x \propto L_{wind}^{0.89 \pm 0.47}$ but the slope is quite uncertain due to scatter in the data. Factors that could contribute to this scatter include uncertainties in distances, X-ray luminosity dereddening corrections, WR star mass-loss rates (which are sensitive to clumping effects), and terminal wind speeds.

A notable outlier is the WN6h star WR 136, which appears to be underluminous in X-rays compared to other WN stars with comparable L_{wind} values (Fig. 5) and to other WN stars with comparable stellar luminosities L_{star} (Fig. 4). Its L_{star} value is also low compared to other WNh stars (Fig. 6 of Hamann et al. 2006). This raises a question as to whether current distance estimates may be too low. The estimates range from $d = 1.26$ kpc (Hamann et al. 2006) to $d = 1.82$ kpc (Nugis & Lamers 2000), whereas our derived X-ray luminosity $\log L_x = 31.51$ ergs s^{-1} is based on the *Hipparcos* distance $d = 1.64$ kpc (S10). We note that there is also a large uncertainty in the L_x value of WR 136 because of poorly-constrained X-ray absorption (N_H) in spectral fits. Some statistically-acceptable spectral models require higher absorption and yield dereddened values as high as $\log L_x \approx 32.2$ ergs s^{-1} ($d = 1.64$ kpc). Such higher values, if correct, would shift the position of WR 136 upward in Figures 4 and 5 (as shown by the L_x error bar), in better agreement with other WN stars.

If the above $L_x \propto L_{wind}$ relation reflects a true physical dependence, then the obvious conclusion would be that a relatively constant fraction of the kinetic energy in WN star winds is being converted into X-ray energy. Interestingly, the MCWS model of Babel & Montmerle (1997a) predicts such a dependence. Specifically, they obtain $L_x \approx \frac{1}{2}\dot{M}v_{shock}^2$, and they infer $v_{shock} \sim v_\infty$ in order to reproduce the X-ray luminosity of the A0p star IQ Aur from their model. Thus, there is some theoretical support for a $L_x \propto L_{wind}$ relation in early-type stars with magnetic fields. Even so, some observational scatter in this relation would be expected due to differences in B-field strengths between stars (eq. [10] of Babel & Montmerle 1997a) and bearing in mind that collision of the two hemispherical wind components could in some cases occur at subterminal speeds. Although the existence of strong surface magnetic fields on single WR stars is not yet established, some WR + OB binaries do exhibit nonthermal radio emission which may be associated with weak magnetic fields above the surface (Abbott et al. 1986; Skinner et al. 1999; Dougherty & Williams 2000). Since the MCWS mechanism operates in single stars there is no need to postulate unseen companions in this interpretation.

If close unseen companions are present in our sample of putatively single WN stars then hot plasma could be created via the colliding wind mechanism. If the WR wind momentum dominates that of the companion, then the CW shock would form at or near the companion surface. This could also give rise to a $L_x \propto L_{wind}$ dependence, but considerable scatter would be expected since in this case the predicted L_x also depends on binary separation and the radius of the companion star (Usov 1992; Luo et al. 1990). Since we have no specific information on the existence of such companions, their stellar or wind properties, or their orbital parameters, a meaningful comparison of the observed L_x values with CW model predictions cannot yet be made.

4.2. High X-ray Plasma Temperatures in WN Stars

All WN stars for which good-quality CCD X-ray spectra exist show a high-temperature plasma component ($kT_{hot} \gtrsim 2$ keV) and almost always a cooler component ($kT_{cool} < 1$ keV). The cool component could be due to radiative instability wind shocks, but the origin of the hotter component is not yet known. Analysis of *XMM* EPIC and *Chandra* ACIS spectra of WN stars reveals a broad range of hot-component temperatures from $kT_{hot} \approx 2$ keV (WR 1, WR 78) up to $kT_{hot} \approx 4 - 8$ keV (WR 20b, WR 110, WR 134; S10).

Such high-temperature plasma could be produced by supersonic WR winds shocking onto denser downstream material, or the wind from the opposite hemisphere (as in the MCWS model), or the wind or surface of as yet undetected companions (CW shocks). These models all predict that the *maximum* shock temperature should scale proportionally with the pre-shock wind-speed as $kT_{shock}^{(max)} \approx 1.96\mu v_{1k}^2$ keV, where μ is the mean atomic weight per particle and v_{1k} is the wind speed in units of 1000 km s^{-1} (Babel & Montmerle 1997a; Luo et al. 1990; Stevens et al. 1992). For solar abundances $\mu \approx 0.6$ but for metal-enriched WN star winds $\mu \approx 1.06$ (van der Hucht et al. 1986). For the WN star case of interest here one thus obtains $kT_{shock}^{(max)} \approx 2v_{\infty,1k}^2$ keV, assuming that the wind has reached terminal speed at the shock interface.

Terminal wind speeds of X-ray detected WN stars lie in the range $v_{\infty} \approx 700 - 2500 \text{ km s}^{-1}$ (Table 2; S10). Thus, the above shock models predict maximum shock temperatures $kT_{shock}^{(max)} \approx 1 - 12$ keV. The values of kT_{hot} determined from X-ray spectra lie comfortably within this range. However, there is no clear trend for a proportionality relation $kT_{hot} \propto v_{\infty}^2$, as one might naively expect from shock-model predictions. The WN star with the lowest v_{∞} for which a good-quality CCD spectrum is available is the WN9ha star WR 79a ($v_{\infty} \approx 955 \text{ km s}^{-1}$, Table 2) and its best-fit temperature is $kT_{hot} = 2.66$ [1.66 - 5.60; 90% conf.] keV (S10). By comparison, the WN4 star WR 1 has a higher terminal speed ($v_{\infty} \approx 1600 - 2135 \text{ km s}^{-1}$; Nugis & Lamers 2000; Ignace et al. 2001; Hamann et al. 2006) but a lower best-fit temperature $kT_{hot} = 1.72$ [1.36 - 2.21; 90% conf.] keV based on our analysis of *XMM* archive data (obsid 0552220101; see also Ignace et al. 2003a for analysis of an earlier *XMM* observation with a shorter exposure).

Given the above results, it is not yet clear that terminal wind speed is the primary parameter governing hot-plasma component temperatures in WN stars. Other factors such as magnetic fields (if present) could play a role in plasma heating. Even if the hot-component plasma temperature is governed by v_{∞} , establishing such a dependence from the existing data will not be straightforward. As noted above, shock models predict that the maximum shock temperature $kT_{shock}^{(max)} \propto v_{\infty}^2$, but shocks will in general produce plasma over a range of temperatures. X-ray spectral fits of CCD spectra using simplistic 2T models only provide

an estimate of the *average* hot-component temperature kT_{hot} , which will in general be less than $kT_{hot}^{(max)}$. Furthermore, the inferred values of kT_{hot} from fits of moderate resolution CCD spectra can be uncertain by a factor of ~ 2 (S10). By comparison, values of v_∞ are typically uncertain by $\approx 10\%$ - 20% . More accurate temperature discrimination is needed to search for any correlation of maximum plasma temperature with wind speed. High-resolution X-ray grating spectra can provide more detailed information on the distribution of X-ray plasma emission measure as a function of temperature. But improvements in X-ray telescope sensitivity will be needed to acquire grating spectra for a sample of WN stars that is sufficiently large to undertake correlation studies.

5. Summary

The main results of this study are the following:

1. We report new X-ray detections of the WNL stars WR 16 (WN8h) and WR 78 (WN7h). These new detections, when combined with previous detections show that X-ray emission is present in all WN subtypes from WN2 - WN9. This contrasts sharply with single carbon-rich WC stars which so far remain undetected in X-rays.
2. The *XMM* detection of WR 16 is of low significance and the emission is too faint for spectral analysis. However, the X-ray spectrum of WR 78 reveals a high-temperature plasma component ($kT_{hot} \approx 2$ keV), similar to that observed in other WN stars. Such hotter plasma is not predicted for X-ray emission arising solely in line-driven instability shocks. The origin of the hot plasma in WN stars is not yet known. Shock models predict that the maximum plasma temperature will scale with terminal wind speed according to $kT_{shock}^{(max)} \propto v_\infty^2$. Such a dependence is not yet seen in the existing data but could be masked because temperatures determined from CCD X-ray spectra are average (not maximum) values and are in many cases uncertain by a factor of ~ 2 .
3. The X-ray luminosities of the WN8 stars WR 16 (a faint detection) and WR 40 (a non-detection) are an order of magnitude less than typical values observed for other detected WN stars. These WN8 stars also have the lowest terminal wind speeds of any WN stars observed so far, suggesting a possible link between terminal wind speed (or a parameter that depends on wind speed) and X-ray luminosity in single WN stars.
4. The two new X-ray detections of WR 16 and WR 78 conform to and strengthen a previously noted trend of increasing L_x with wind luminosity $L_{wind} = \frac{1}{2}Mv_\infty^2$ in WN stars. A regression fit based on existing data for 11 WN stars gives $L_x \propto L_{wind}^{0.89 \pm 0.47}$ and

a correlation test yields a correlation probability $P_{corr} = 0.93$. This trend needs to be confirmed in a larger sample of WN stars but tentatively suggests that wind kinetic energy may be an important factor in governing the X-ray luminosity levels of WN stars.

This work was supported by NASA/GSFC award NNX09AR25G. This work was based on observations obtained with *XMM-Newton*, an ESA science mission with instruments and contributions directly funded by ESA member states and the USA (NASA). SZ acknowledges financial support from Bulgarian National Science Fund grant DO-02-85.

Table 1. XMM-Newton Observations (WNL Stars)

Parameter	WR 16	WR 78
Date	2009 Dec. 28-29	2010 Mar. 2-3
ObsId	0602020301	0602020201
Start Time (UTC)	19:57:31	14:08:02
Stop Time (UTC)	06:35:01	00:45:08
Optical Filter	medium	thick
pn exposure (ks) ^a	30.0	26.3
MOS exposure (ks) ^a	33.0	26.5

^aUsable exposure after removing high-background time intervals. MOS exposure is per MOS. The total exposure times before removing high-background intervals were 37.4 ks (WR 16), 37.5 ks (WR 78).

Table 2. WNL Star Properties^a

Name	Sp. Type	d (kpc)	A _V (mag)	v _∞ (km/s)	log \dot{M} (M _⊙ /yr)	log L _{star} (L _⊙)
WR 16	WN8h	3.60 (2.37 - 4.36)	1.67	670 (630 - 740)	−4.35 (−4.55 - −4.20) ^b	5.8 (5.50 - 6.15)
WR 78	WN7h	2.00 (1.58 - 2.00)	1.55	1375 (1365 - 1385)	−4.25 (−4.42 - −4.10) ^c	5.9 (5.63 - 6.20)
WR 79a	WN9ha	1.99	1.28	955	−4.60 (−4.57 - −4.62) ^d	5.78

^a Spectral types are from van der Hucht (2001). Data for WR 16 and WR 78 show the values adopted in this study followed in parentheses by the range of values quoted in the literature (Crowther et al. 1995; Nugis & Lamers 2000; van der Hucht 2001; Hamann et al. 2006). Data for WR 79a are from Crowther & Bohannon (1997).

^bClumping-corrected values are log \dot{M} = −4.55 at d = 3.93 kpc from radio data (Nugis & Lamers 2000) and log \dot{M} = −4.3 from empirical relations (Hamann et al. 2006).

^cClumping-corrected values are log \dot{M} = −4.42 at d = 1.58 kpc from radio data (Nugis & Lamers 2000) and log \dot{M} = −4.2 from empirical relations (Hamann et al. 2006).

^dRadio-derived and spectroscopic values are in good agreement, and clumping effects are thought to be small in WR 79a (Crowther & Bohannon 1997).

Table 3. WNL Star X-ray Source Properties^a

Name	R.A. (J2000)	Decl. (J2000)	Counts ^b (cts)	Rate (cts/ks)	E ₅₀ (keV)	P _{cons}	log L _x ^c (ergs/s)	Identification(offset) (arcsec)
WR 16	09 54 52.94	−57 43 39.2	31±6	1.03±0.20	... ^d	... ^d	31.14	GSC J095452.90−574338.27 (0.96)
WR 78	16 52 19.18	−41 51 15.8	800±28	30.5±1.10	2.47	0.12 (0.97)	32.84	GSC J165219.25−415116.25 (0.93)
WR 79a ^e	16 54 58.52	−41 09 02.9	805±29	23.0±0.83	1.35	0.63 (0.33)	32.14	GSC J165458.50−410903.08 (0.30)

^a Notes: *XMM-Newton* data are from EPIC pn. Parameters were determined using events in the 0.3 - 8 keV range. Tabulated quantities are: source name, J2000.0 X-ray position (R.A., Decl.), pn net counts and net counts error (background-subtracted), pn count rate (Rate) obtained by dividing net counts by the usable exposure times given below, median photon energy E₅₀, probability of constant count-rate (P_{cons}) from the KS test followed in parentheses by the value determined from χ^2 analysis of background-subtracted binned light curves using 1000 s bins, unabsorbed X-ray luminosity L_x (0.3 - 8 keV) assuming the distances in Table 2, and HST GSC v2.3.2 optical counterpart identification. The offset (in arcsecs) between the X-ray and optical counterpart position is given in parentheses. The values of E₅₀ and P_{const} were evaluated using events within an extraction circle of radius 15'' (68% encircled energy) in order to minimize background effects. Usable pn exposure times after removing high-background intervals were: 30.0 ks (WR 16), 26.26 ks (WR 78), and 35.03 ks (WR 79a).

^bNet counts for WR 78 and WR 79a are based on background-subtracted events within an extraction circle of radius 45'' (90% encircled energy). A smaller extraction region of radius 15'' (68% encircled energy) was used for the faint source WR 16 to minimize background contribution.

^cUnabsorbed L_x values for WR 78 and WR 79a are based on fluxes measured in spectral fits after resetting the column density to zero (N_H = 0) for all model components. The value for WR 16 is based on a PIMMS simulation (Sec. 3.1).

^dInsufficient counts for a reliable measurement.

^eSee Skinner et al (2010) for additional information on WR 79a.

Table 4. X-ray Spectral Fits of WR 78

Parameter	Value
Model	$N_{H,1} * kT_1 + N_{H,2} * kT_2$
Abundances ^a	WN
$N_{H,1}$ (10^{22} cm ⁻²)	1.38 [1.20 - 1.60]
kT_1 (keV)	0.64 [0.48 - 0.88]
norm ₁ (10^{-6})	3.59 [2.40 - 6.30]
$N_{H,2}$ (10^{22} cm ⁻²)	6.55 [4.10 - 10.7]
kT_2 (keV)	2.27 [1.63 - 2.90]
norm ₂ (10^{-6})	14.5 [8.30 - 34.4]
χ^2/dof	49.2/51
χ^2_ν	0.96
F_X (10^{-13} ergs cm ⁻² s ⁻¹)	2.15 (14.5)
$F_{X,1}$ (10^{-13} ergs cm ⁻² s ⁻¹)	0.33 (4.27)
log L_X (ergs s ⁻¹)	32.84
log [L_X/L_{star}]	-6.64
log [L_X/L_{wind}]	-4.68

Note. — Based on simultaneous XSPEC (vers. 12.4.0) fit of the background-subtracted pn, MOS1, MOS2 spectra binned to a minimum of 20 counts per bin using the optically thin thermal plasma *vapex* model. All models included the XSPEC *wabs* photoelectric absorption component, based on Morrison & McCammon (1983) cross-sections and Anders & Ebihara (1982) relative abundances. The tabulated parameters are total equivalent neutral H absorption column density (N_H) including both ISM and local stellar (e.g. wind) contributions, the product of Boltzmann’s constant time plasma temperature (kT), and XSPEC component normalization (norm). Square brackets enclose 90% confidence intervals. The total X-ray flux (F_X) and flux of the cool component ($F_{X,1}$) are the absorbed values in the 0.3 - 8 keV range, followed in parentheses by unabsorbed values. The unabsorbed luminosity L_X (0.3 - 8 keV) assumes $d = 1.99$ kpc (Table 2). L_{star} and $L_{wind} = (1/2)\dot{M}v_\infty^2$ are from Table 2.

^aAbundances were held fixed at the generic WN values given in Table 1 of Van der Hucht et al. (1986). The generic WN abundances reflect H depletion and N enrichment and are by number: He/H = 14.9, C/H = 1.90E-03, N/H = 9.36E-02, O/H = 4.35E-03, Ne/H = 9.78E-03, Mg/H = 3.26E-03, Si/H = 3.22E-03, P/H = 1.57E-05, S/H = 7.60E-04, Fe/H = 1.90E-03. All other elements were held fixed at solar abundances (Anders & Grevesse 1989).

REFERENCES

- Abbott, D.C., Biegging, J.H., Churchwell, E., & Torres, A.V. 1986, *ApJ*, 303, 239
- Anders, E., & Ebihara, M. 1982, *Geochim. Cosmochim. Acta*, 46, 2363
- Anders, E., & Grevesse, N. 1989, *Geochim. Cosmochim. Acta*, 53, 197
- Antokhin, I., Bertrand, J.-F., Lamontagne, R., & Moffat, A.F.J. 1995, *AJ*, 109, 817
- Babel, J. & Montmerle, T., 1997a, *A&A*, 323, 121
- Babel, J. & Montmerle, T., 1997b, *ApJ*, 485, L29
- Berghöfer, T.W., Schmitt, J.H.M.M., Danner, R., & Cassinelli, J.P., 1997, *A&A*, 322, 167
- Bratschi, P. & Blecha, A. 1996, *A&A*, 313, 537
- Cassinelli, J.P., Miller, N.A., Waldron, W.A., MacFarlane, J.J., & Cohen, D.H., 2001, *ApJ*, 554, L55
- Chen, W. & White, R.L. 1991, *ApJ*, 366, 512
- Crowther, P.A. 2007, *ARA&A*, 45, 177
- Crowther, P.A. & Bohannan, B. 1997, *A&A*, 317, 532
- Crowther, P.A., Smith, L.J., Hillier, D.J., & Schmutz, W. 1995, *A&A*, 293, 427
- Dougherty, S.M. & Williams, P.M. 2000, *MNRAS*, 319, 1005
- Feldmeier, A., Kudritzki, R.-P., Palsa, R. Pauldrach, A.W.A., & Puls, J., 1997, *A&A*, 320, 899
- Gagné, M. et al. 2005, *ApJ*, 628, 986
- Gayley, K.G. & Owocki, S.P., 1995, *ApJ*, 446, 801
- Gorenstein, P. 1975, *ApJ*, 198, 95
- Gosset, E., Nazé, Y., Claeskens, J.-F., Rauw, G., Vreux, J.-M., & Sana, H. 2005, *A&A*, 429, 685
- Hamann, W.-R., Gräfener, G. & Liermann, A. 2006, *A&A*, 457, 1015
- Howarth, I.D. & Schmutz, W. 1992, *A&A*, 261, 503

- Ignace, R., Cassinelli, J.P., Quigley, M., & Babler, B. 2001, *ApJ*, 558, 771
- Ignace, R., Oskinova, L.M., & Brown, J.C. 2003a, *A&A*, 408, 353
- Ignace, R., Quigley, M.F., & Cassinelli, J.P. 2003b, *ApJ*, 596, 538
- Kahn, S.M. et al., 2001, *A&A*, 365, L312
- Lucy, L.B., 1982, *ApJ*, 255, 286
- Lucy, L.B. & White, R.L., 1980, *ApJ*, 241, 300
- Luo, D., McCray, R., & MacLow, M-M., 1990, *ApJ*, 362, 267
- Manfroid, J., Gosset, E., & Vreux, J.M. 1987, *A&A*, 185, L7
- Marston, A.P., Welzmler, J., Bransford, M.A., Black, J.H., & Bergman, P. 1999, *ApJ*, 518, 769
- Moffat, A.F.J. & Niemela, V.S. 1982, *A&A*, 108, 326
- Morrison, R. & McCammon, D. 1983, *ApJ*, 270, 119
- Nazé, Y. 2009, *A&A*, 506, 1055
- Nugis, T. & Lamers, H.J.G.L.M. 2000, *A&A*, 360, 227
- Owocki, S.P., Sundqvist, J., Cohen, D., & Gayley, K. 2011, in *Four Decades of Research on Massive Stars*, eds. L. Drissen, C. Robert, & N. St.-Louis (San Francisco: ASP), in press
- Pollock, A.M.T. 1987, *ApJ*, 320, 283
- Pollock, A.M.T., Corcoran, M.F., Stevens, I.R., & Williams, P.M. 2005, *ApJ*, 629, 482
- Prilutskii, O.F. & Usov, V.V. 1976, *Soviet Ast.*, 20, 2
- Sanders, W.T., Cassinelli, J.P., Myers, R.V., & van der Hucht, K.A. 1985, *ApJ*, 288, 756
- Schild, H. et al. 2004, *A&A*, 422, 177
- Seward, F.D., Forman, W.R., Giacconi, R., Griffiths, R.E., Harnden, F.R., Jones, C., & Pye, J.P. 1979, *ApJ*, 234, 55
- Skinner, S.L., Güdel, M., Schmutz, W., & Stevens, I.R., 2001, *ApJ*, 558, L113

- Skinner, S.L., Güdel, M., Schmutz, W., & Zhekov, S. 2006, *Astrophys. Space Sci.*, 304, 97
- Skinner, S.L., Itoh, M., Nagase, F., & Zhekov, S.A. 1999, *ApJ*, 524, 394
- Skinner, S.L., Sokal, K.R., Cohen, D.H., Gagné, M., Owocki, S.P., & Townsend, R.H. 2008, *ApJ*, 683, 796
- Skinner, S.L., Zhekov, S., Güdel, M., & Schmutz, W. 2002, *ApJ*, 572, 477
- Skinner, S.L., Zhekov, S., Güdel, M., & Schmutz, W., & Sokal, K. 2010, *AJ*, 139, 825 (S10)
- Sokal, K.R., Skinner, S.L., Zhekov, S.A., Güdel, M., & Schmutz, W. 2010, *ApJ*, 715, 1327
- Stevens, I.R., Blondin, J.M., & Pollock, A.M.T., 1992, *ApJ*, 386, 265
- Strüder, L. et al., 2001, *A&A*, 365, L18
- Turner, M.J.L. et al., 2001, *A&A*, 365, L27
- ud-Doula, A. & Owocki, S.P., 2002, *ApJ*, 576, 413
- Usov, V.V. 1992, *ApJ*, 389, 635
- van der Hucht, K.A. 2001, *New Ast. Rev.*, 45, 135
- van der Hucht, K.A., Cassinelli, J.P., & Williams, P.M., 1986, *A&A*, 168, 111 (VCW86)
- Vreux, J.M., Magain, P., Manfroid, J., & Scufflaire, R. 1987, *A&A*, 180, L17
- Vuong, M.H., Montmerle, T., Grosso, N., Feigelson, E.D., Verstraete, L., & Ozawa, H. 2003, *A&A*, 408, 581
- Waldron, W.L. & Cassinelli, J.P. 2007, *ApJ*, 668, 456
- Wessolowski, U. 1996, in *Röntgenstrahlung from the Universe (MPE Report 263)*, eds. H.U. Zimmerman, J.E. Trümper, & H. York (Garching: Max-Planck-Inst. für Extraterrestrische Physik), 75
- Zhekov, S.A. & Park, S. 2010, *ApJ*, 721, 518

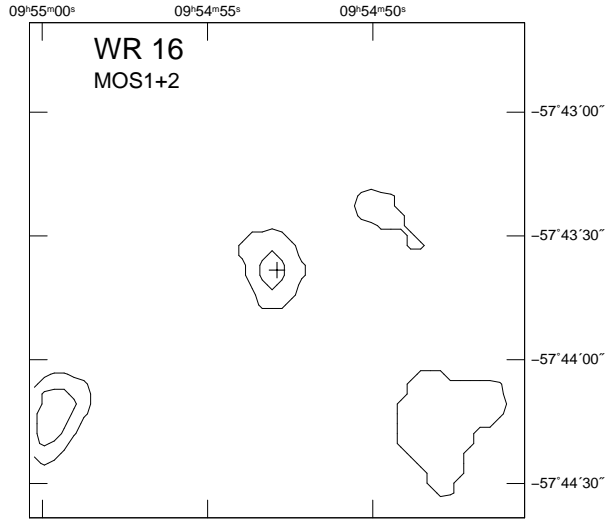


Fig. 1.— Summed EPIC MOS1+2 contour image of WR 16 (0.3 - 8 keV; 33 ks of usable exposure per MOS; Gaussian-smoothed). The inner contour (2σ) encloses a weak excess at the HST GSC stellar position (cross).

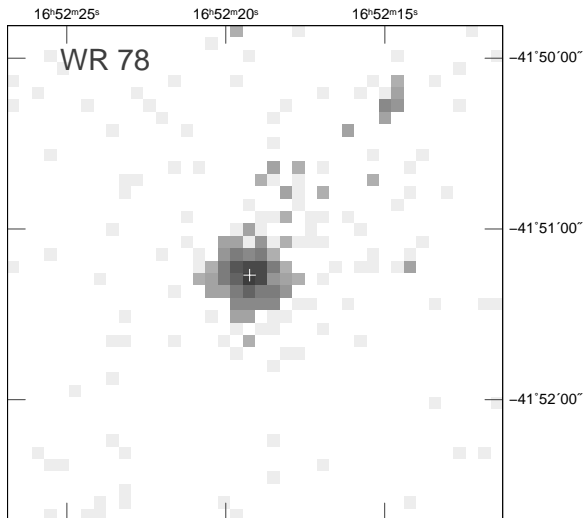


Fig. 2.— EPIC pn image of WR 78 (0.3 - 8 keV; 26.3 ks of usable exposure; 4."3 pixels) showing a clear detection at the HST GSC stellar position (cross).

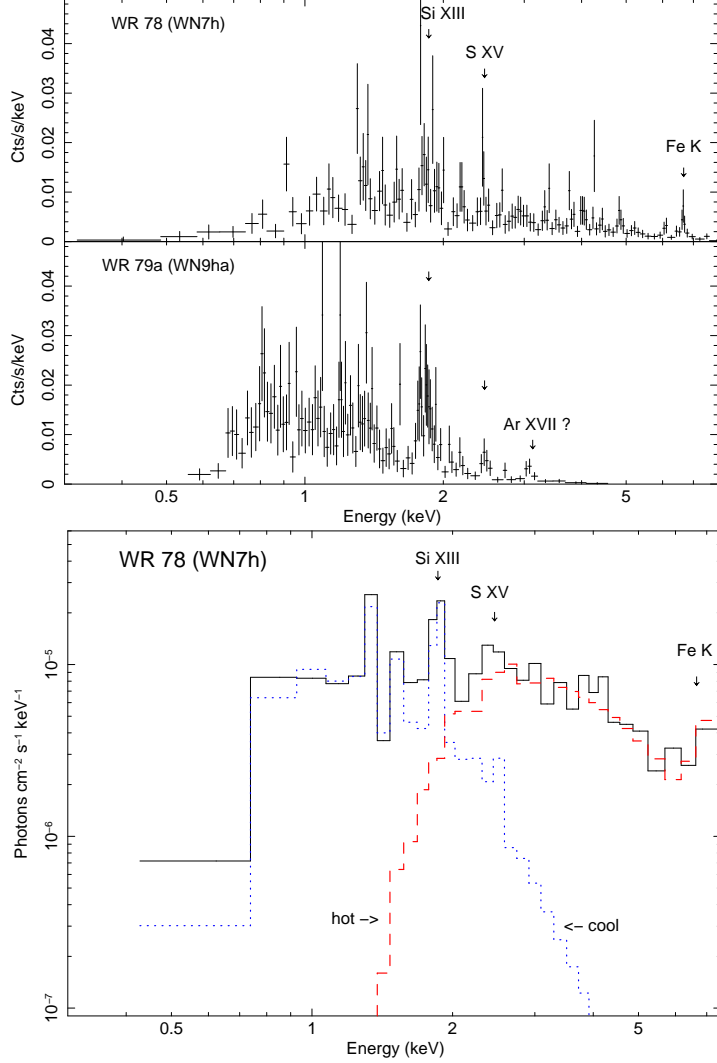


Fig. 3.— Top and Middle: EPIC pn background-subtracted spectra of WR 78 and WR 79a, binned to a minimum of 5 counts per bin. Spectral fit parameters for WR 78 are given in Table 4. Best-fit parameters for WR 79a are $N_{\text{H}} = 7.5 [6.4 - 8.3] \times 10^{21} \text{ cm}^{-2}$, $kT_1 = 0.55 [0.46 - 0.61] \text{ keV}$, and $kT_2 = 2.66 [1.66 - 5.60] \text{ keV}$ where brackets enclose 90% confidence ranges (S10). Bottom: Unfolded spectrum of WR 78 binned to a minimum of 20 counts per bin showing the separate contributions of the cool (dotted line) and hot (dashed line) components (Table 4). The hot component accounts for most of the emission above 2 keV including the high-temperature Fe K line. Error bars omitted for clarity; log-log scale.

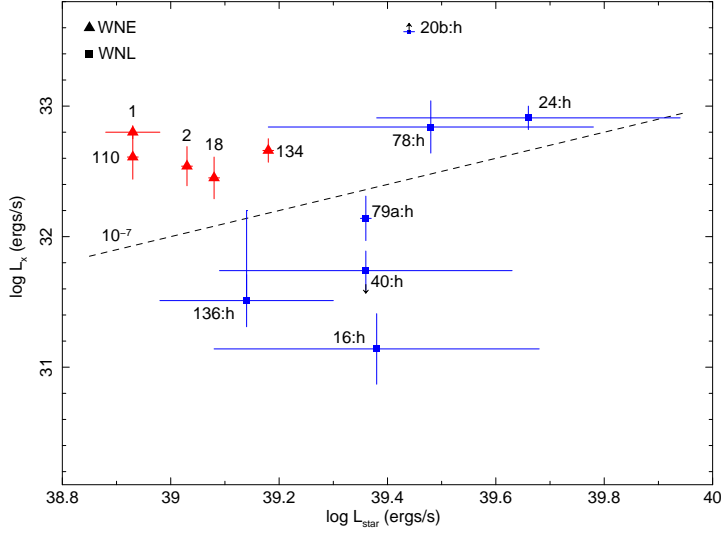


Fig. 4.— Unabsorbed X-ray luminosity (0.3 - 8 keV) versus stellar luminosity for WN stars. Assumed distances are given in Table 2 and S10. WR star numbers are from van der Hucht 2001 and :h following the number denotes the presence of hydrogen in the spectrum. WNE and WNL classifications follow Hamann et al. 2006. Unabsorbed L_x was obtained by setting the column density to zero ($N_H = 0$) in best-fit spectral models and measuring the unabsorbed flux. Exceptions are the faint source WR 16 (PIMMS simulations; Sec. 3.1) and the undetected star WR 40. Unabsorbed L_x values are from this work (WR 16, WR 78), Skinner et al. 2002 (WR 110), and Skinner et al. 2010 (and references therein). The L_x value for WR 1 is based on analysis of *XMM* archive data (obsid 0552220101) and assumes $d = 1.82$ kpc (van der Hucht 2001). The L_x upper limit for WR 40 is from Gosset et al. 2005, adjusted upward by 0.14 dex to allow for distance uncertainties. L_{star} uncertainties reflect the range of values published in the literature (Crowther et al. 1995; Crowther & Bohannan 1997; Nugis & Lamers 2000; Hamann et al. 2006). The dashed line shows the canonical $L_x = 10^{-7}L_{bol}$ relation for O and early B-type stars. The spectral types from van der Hucht (2001) are: WR 1 (WN4), WR 2 (WN2), WR 16 (WN8h), WR 18 (WN4), WR 20b (WN6:h), WR 24 (WN6ha), WR 40 (WN8h), WR 78 (WN7h), WR 79a (WN9ha), WR 110 (WN5), WR 134 (WN6), WR 136 (WN6h).

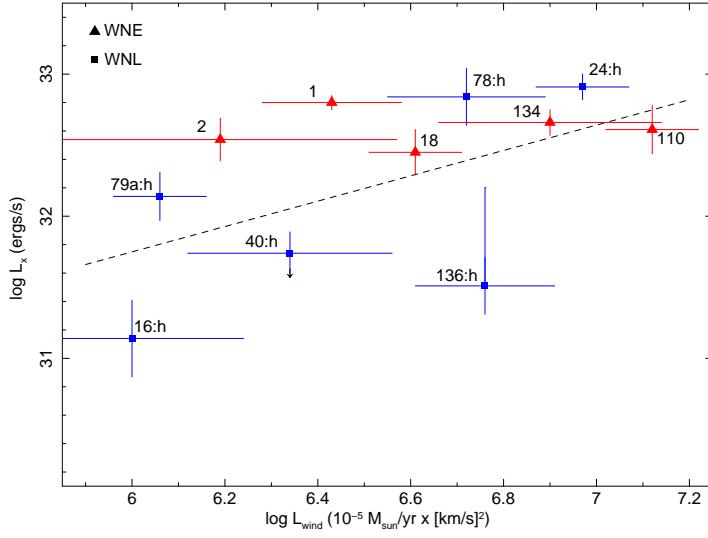


Fig. 5.— Unabsorbed X-ray luminosity (0.3 - 8 keV) versus wind luminosity $L_{wind} = \frac{1}{2}\dot{M}v_{\infty}^2$ for WN stars. Mass-loss data are based on published values (see references below) and uncertainties reflect the range of published values. WR 20b is excluded for lack of reliable mass-loss data. The dashed line shows a linear regression fit $\log L_x = 0.89(\pm 0.47)\log L_{wind} + 26.41(\pm 0.55) \text{ ergs s}^{-1}$. Symbols and spectral types are the same as given in Figure 4. Mass-loss parameter references (in parentheses): WR 1: (4,7,10) WR 2: (1,2,4,8) WR 16: (3,4,10); WR 18: (4); WR 24: (3,4,10); WR 40: (3,4,9,10) WR 78: (3,4,10); WR 79a: (5); WR 110: (4); WR 134: (1,4,10); WR 136: (1,2,4,6,7,10). *References:* (1) Abbott et al. 1986; (2) Howarth & Schmutz 1992; (3) Crowther et al. 1995; (4) Hamann et al. 2006; (5) Crowther & Bohannan 1997; (6) Ignace et al. 2001; (7) Ignace et al. 2003b; (8) van der Hucht 2001; (9) Gosset et al. 2005; (10) Nugis & Lamers 2000.